

AERODYNAMIC HEATING OF THE BRAZILIAN 14-X HYPERSONIC WAVERIDER SCRAMJET VEHICLE AT MACH NUMBERS 7 AND 10

Felipe Jean da Costa, felipejean@ieav.cta.br

ITA - Instituto Tecnológico de Aeronáutica, Praça Marechal Eduardo Gomes, nº 50 Vila das Acácias CEP. 12.228-900 São José dos Campos, SP - Brasil

Tiago Cavalcanti Rolim, tiagorolim@ieav.cta.br

Israel da Silva Rêgo, israel.rego@ieav.cta.br

Marco Antônio Sala Minucci, marco.salaminucci@gmail.com

Antônio Carlos de Oliveira, acoc@ieav.cta.br

Paulo Gilberto de Paula Toro, toro@ieav.cta.br

IEAv - Instituto de Estudos Avançados, Trevo Coronel Aviador José Alberto Albano do Amarante, nº 1 Putim CEP. 12.228-001 São José dos Campos, SP - Brasil

Abstract. The Brazilian 14-X Hypersonic waverider scramjet Aerospace Vehicle, designed at the Prof. Henry T. Nagamatsu Laboratory of Aerothermodynamics and Hypersonics, at the Institute for Advanced Studies, is a technological demonstrator endowed with waverider technology, to obtain lift due to conical/oblique shockwave during the hypersonic flight; and hypersonic airbreathing propulsion system based on supersonic combustion (scramjet), to fly in the Earth's atmosphere at 30 km altitude at speeds corresponding to the Mach numbers 7 and 10. During high speed flight the shock waves and the viscous forces yield the phenomenon called aerodynamic heating, where his physical meaning is the friction between the fluid filaments and the body or compression at the stagnation regions of the leading edge that converts the kinetic energy into heat within a thin layer of air which blankets the body. The temperature of this layer increases with the square of the speed. This high temperature is concentrated in the boundary-layer, where heat will flow readily from the boundary-layer to the hypersonic aerospace vehicle structure. Fay and Riddell and Eckert methods are applied to the stagnation point and to the flat plate segments in order to calculate the aerodynamic heating, which the results will be presented from the leading edge to the trailing edge of the Brazilian 14-X Hypersonic waverider scramjet Aerospace Vehicle at Mach numbers 7 and 10.

Keywords: 14-X, Aerodynamic heating, scramjet, hypersonics, waverider

1. THE BRAZILIAN 14-X HYPERSONIC AEROSPACE VEHICLE

The Laboratory of Aerothermodynamics and Hypersonics Prof. Henry T. Nagamatsu, at the Institute for Advanced Studies, is developing the 14-X Hypersonic Aerospace Vehicle, 14-X waverider (Figure 1). The 14-X waverider is a technological demonstrator designed to demonstrate, during the hypersonic flight speed corresponding to Mach number 10 through the Earth's atmosphere at 30 km altitude, two innovative technologies: waverider technology, to obtain lift from conical shock wave during the supersonic or hypersonic flight; and the scramjet engine that consists in a hypersonic airbreathing propulsion system based on supersonic combustion (Costa, 2014).

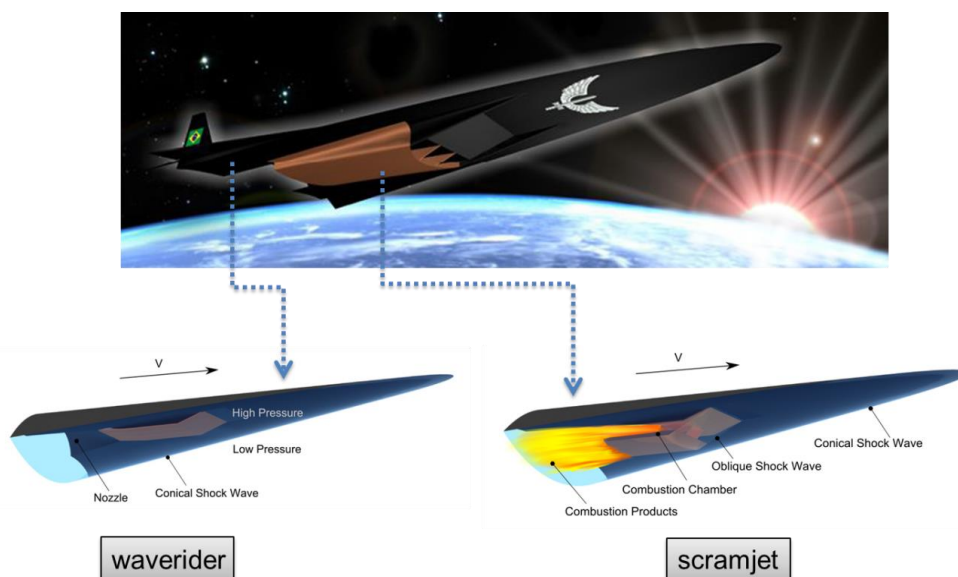


Figure 1. The 14-X Hypersonic Aerospace Vehicle with waverider and scramjet concepts

The scramjet engine during the hypersonic flight promotes the compression and deceleration of freestream atmospheric air, at the inlet of the scramjet, using the oblique/conical shock waves. The scramjet is integrated to the vehicle to obtain the adequate air in supersonic speed conditions to burn fuel (in general, Hydrogen) in the combustion chamber. The scramjet engine is an aeronautical engine without moving parts, and due this fact it is necessary another propulsion system to accelerate the vehicle powered by scramjet up to operation conditions. Rocket engines represent the best solution, in technical and economic terms, to launch the powered vehicle by scramjet. The Brazilian two-stage rocket engines (S31 and S30) will accelerate the VHA 14-X to the predetermined conditions of the operation of the scramjet at 30 km altitude, but at Mach number 7 (the maximum corresponding speed that S31 and S30 reaches).

2. AERODYNAMIC HEATING

When the air reaches high speeds, during supersonic/hypersonic flights, it is decelerated by shock waves and by viscous forces in the boundary layer. This deceleration yields the phenomenon called aerodynamic heating. The aerodynamic heating consist in the friction between the fluid filaments and the body or the compression at the stagnation regions of leading edge that convert the kinetic energy into heat within a thin layer of air which blankets the body. The temperature of this layer increases with the square of the speed of the vehicle, and this high temperature is concentrated in the boundary-layer, where heat will flow readily from the boundary-layer to the hypersonic aerospace vehicle surface (van Driest, 1956). Due the high static temperature in the shock layer, the aerodynamic heating is affected by a possible dissociation and ionization of the air that occurs at finite rates, and implies that the thermochemical equilibrium cannot be achieved in the flow field (Fay and Riddell, 1958). Furthermore, the atoms and ions release a high specific energy, if they are diffused on the surface and consequently recombined at the wall, which causes a significantly increase in the heat transferred by conventional molecular conduction. Using a non-catalytic surface will be possible to eliminate the fraction of heat transfer that is transported by atomic diffusion into the wall followed by recombination at the surface. Although, to an effective use of a non-catalytic surface, the atoms cannot recombine firstly in the gas before reaching the wall. If the wall is catalytic, the concentration of atom is reduced to the equilibrium value of the wall temperature. If the atoms recombine in the boundary layer or at the wall there will be no major effect on convective heat transfer (Fay and Riddell, 1958).

For the aerodynamic heating are applied two theories, the Fay and Riddell theory to the stagnation point due the existence of a blunted nose formed at the vehicle's leading edge during the manufacturing process; and the Eckert's reference enthalpy theory applied to the vehicle's surface assuming the air flow in the conical surfaces as a flow over a flat plate.

2.1 Fay and Riddell Aerodynamic Heating at Stagnation Point Theory

The theory of stagnation point heat transfer in dissociated air developed by Fay and Riddell considers the effects of diffusion and of atom recombination in the boundary layer. The boundary-layer equations, at the stagnation point, can be reduced exactly to a set of nonlinear ordinary differential equations (self-similar boundary-layer equations) even when the chemical reactions proceed so slowly that the boundary layer not achieve the thermochemical equilibrium. They considered the energy transport through a motionless dissociated gas with temperature and concentration gradients.

The convective heat flux at the stagnation point may be given by:

$$\dot{q}_w = \left[\frac{k}{\bar{c}_p} \frac{\partial h}{\partial y} \right]_w + \left[\sum \left(\frac{k}{\bar{c}_p} \right) \left(h_i - h_i^0 \right) \left\{ \left(L_i - 1 \right) \left(\frac{\partial c_i}{\partial y} \right) + \left(\frac{L_i^T c_i}{T} \right) \left(\frac{\partial T}{\partial y} \right) \right\} \right]_w \quad (1)$$

where, k , \bar{c}_p , h , T are thermal conductivity, specific heat per unit mass at constant pressure considering translation, rotation and vibration, enthalpy per unit of mass of mixture, absolute temperature, respectively. The subscript w indicates the condition on the wall. c_i is mass fraction of component i . L_i and L_i^T are the Lewis number and thermal Lewis number, respectively, given by $L_i = D_i \frac{\rho \bar{c}_p}{k}$ and $L_i^T = D_i^T \frac{\rho \bar{c}_p}{k}$, where D_i and D_i^T are diffusion coefficient and thermal diffusion coefficient, respectively.

Fay and Riddell present the following similarity, which includes the usual Howarth and Mangler transformations of independent variables x and y , as proposed by Lees given by:

$$\eta = \frac{r u_e}{\sqrt{2 \xi}} \int_0^y \rho dy \quad (2)$$

$$\xi = \int_0^x \rho_w \mu_w u_e r_0^{2k} dx \quad (3)$$

Further, some dimensionless dependent variables were used for them and are given by:

$$g = \frac{h + u^2/2}{h_s} \quad \theta = \frac{T}{T_e} \quad s_i = \frac{c_i}{c_{ie}} \quad (4)$$

where, subscripts e refers to the free stream condition and s refers to the free stream condition at the stagnation point.

The convective heat flux at the stagnation point equation in terms of the dimensionless temperature and enthalpy distributions can be written as follow:

$$\dot{q}_w = \left[2 \left(\frac{\rho}{\mu} \right)_w \left(\frac{du_e}{dx} \right)_s \right]^{1/2} \frac{k_w h_s}{c_{pw}} \left[g_\eta + \sum c_{ie} \left(\frac{h_i - h_i^0}{h_s} \right) \left\{ (L_i - 1) s_{i\eta} + L_i^T s_{i\eta} \frac{\theta_\eta}{\theta} \right\} \right]_w \quad (5)$$

where $s_{i\eta} = \frac{\partial s_i}{\partial \eta}$, $\theta_\eta = \frac{\partial \theta}{\partial \eta}$, and $g_\eta = \frac{\partial g}{\partial \eta}$, respectively. Also ρ , μ , $\left(\frac{du_e}{dx} \right)_s$ are the density, dynamic viscosity, and the velocity gradient at the stagnation point, respectively.

Therefore, the heat transfer at the stagnation point in dissociated air presented by Fay and Riddell is given by:

$$\dot{q}_w = \frac{0.763}{(\text{Pr}_w)^{0.6}} (\rho_e \mu_e)^{0.4} (\rho_w \mu_w)^{0.1} [(h_o)_e - h_w] \left[1 + (Le^{0.52} - 1) \frac{h_d}{(h_o)_e} \right] \left[\left(\frac{du_e}{dx} \right)_t \right]^{0.5} \quad (6)$$

where, the velocity gradient $\left(\frac{du_e}{dx} \right)_s$ may be defined using the Newtonian modified theory for the stagnation point, and is given by

$$\left(\frac{du_e}{dx} \right)_s = \frac{1}{R_N} \sqrt{\frac{2(p_e - p_\infty)}{\rho_e}} \quad (7)$$

where, R_N is the nose radius, p_e , ρ_e , p_∞ , are the pressure and density outside of the boundary layer, and pressure at the freestream, respectively.

2.2 Eckert's Reference Enthalpy Theory

In the literature we can found several methods to calculate the heat transfer and skin friction in high speed boundary layers (Nielsen, 1955), remarkably the mean-enthalpy method to laminar boundary layers used by Rubesin and Johnson (1949), that was applied to turbulent boundary layers by Sommer and Short (1955). Subsequently, Eckert developed the reference enthalpy method assuming that the global effects of the boundary layer with varying properties can be replaced by the boundary layer with constant properties, that corresponds to average properties or at the reference enthalpy (or temperature), which can be found a priori (Heiser and Pratt, 1995).

The convective heat flux for thermal boundary layer with variable properties can be given by the product of the conductance (Stanton number) and an enthalpy difference, as shown by the following equation:

$$q_w = St \cdot \rho_e V_e (h_{aw} - h_w) \quad (8)$$

where, ρ_e and V_e are the density and velocity of the gas in adjacent inviscid flow outside the boundary layer, respectively. h_{aw} and h_w correspond to the adiabatic wall enthalpy and wall enthalpy, respectively. The Stanton number (St), for laminar flow, corresponds to a dimensionless coefficient given by

$$St = \frac{0.332}{Pr^{3/2} Re^{1/2}} \quad (9)$$

where, Pr and Re are Prandtl number and Reynolds number, respectively.

Considering the perfect gas assumption, we may replace the adiabatic wall enthalpy and wall enthalpy, h_{aw} and h_w by:

$$h = c_p \cdot T \quad (10)$$

Therefore, the adiabatic wall temperature may be calculated by the following equation:

$$T_{aw} = T_e \cdot [1 + r \cdot \frac{\gamma-1}{2} \cdot M_e^2] \quad (11)$$

where the recovery factor r , is the ratio of the adiabatic wall enthalpy and total enthalpy related by the kinetic energy. Due to finite thermal conductivity for real gas, part of the thermal energy is conducted away from the higher temperature region of the wall to the gas at low temperature, thus lowering the h_{aw} , and the recovery factor is given by

$$r = \frac{h_{aw} - h_e}{V_e} \quad (12)$$

For laminar and turbulent flows the recovery factor r may be obtained by:

$$r = \begin{cases} \sqrt{Pr} & \text{for laminar} \\ \sqrt[3]{Pr} & \text{for turbulent} \end{cases} \quad \text{where } Pr = \frac{\mu c_p}{k} \quad (13)$$

Therefore, the convective heat flux for thermal boundary layer with variable properties can be given by

$$q_w = \frac{0.332}{Pr^{3/2} Re^{1/2}} \cdot \rho_e V_e (h_{aw} - h_w) \quad (14)$$

Assuming perfect gas the convective heat flux for thermal boundary layer with variable properties can be given by

$$q_w = \frac{0.332}{Pr^{3/2} Re^{1/2}} \cdot \frac{\rho_e V_e}{c_p} (T_{aw} - T_w) \quad (15)$$

Considering the Eckert's reference enthalpy method, the reference temperature T^* is given by

$$T^* = T_e + 0.5(T_w - T_e) + 0.22r(T_s - T_e) \quad (16)$$

where, T_e is the flow temperature after the normal shock wave and T_w is the wall temperature, and the stagnation temperature (T_s) is calculated by:

$$T_s = T_e [1 + \frac{\gamma-1}{2} \cdot M_e^2] \quad (17)$$

where, M_e is the Mach number after the normal shock wave.

The recovery factor r , shown in Eq. 13, is calculated from the Prandtl number valuated at T^* .

To obtain the T^* , firstly the stagnation temperature from Eq. 17 need to be calculated and assume a value for T^* , then calculate Pr^* through Eq. 13. By Sutherland's law (Eq. 18) the reference dynamic viscosity (μ^*) is given, the reference thermal conductivity (k^*), given by Eq. 19, is estimated, and using the software HAP (Hypersonic Airbreathing Propulsion) the reference specific heat at constant pressure (c_p^*) is computed. The recovery factor is

obtained from Eq. 13 and then used to calculate the reference temperature (T^*) from Eq. 16. Once obtained the new T^* , the new Pr^* is calculated through Eq. 13 and then a second T^* using the same Eq. 16. Repeat the whole process until the T^* results converge.

$$\mu^* = 1.46 \cdot 10^{-6} \left(\frac{T^{*1.5}}{T^* + 111} \right) \quad 18$$

$$k^* = 1.993 \cdot 10^{-6} \left(\frac{T^{*1.5}}{T^* + 112} \right) \quad 19$$

Once the reference temperature T^* has been computed, it is possible to proceed to calculate the heat transfer given by:

$$q_w = \frac{0.332 \rho_e u_e (h_{aw} - h_w)}{\frac{1/2}{Pr^{3/2} Re_x}} \quad 20$$

The enthalpy at the adiabatic wall (h_{aw}) is calculated by:

$$h_{aw} = h_e + r \frac{u_e^2}{2} \quad 21$$

where, u_e is the flow velocity and h_e is the flow enthalpy, given by:

$$h_e = c_p T_e \quad 22$$

where, c_p is the specific heat at constant pressure and T_e is the flow temperature after the normal shock.

Similarly to the flow enthalpy, the enthalpy at the wall (h_w) is calculated utilizing:

$$h_w = c_p T_w \quad 23$$

where, T_w is the wall temperature.

The reference Reynolds number (Re^*) is given by:

$$Re^* = \frac{\rho^* u_e x}{\mu^*} \quad 24$$

where, u_e is the flow velocity and x is the surface extension. The reference density (ρ^*) is given by the perfect gas relation, i.e.,

$$\rho^* = \frac{p_2}{RT^*} \quad 25$$

where, p_2 is the flow pressure, R is the air gas constant and T^* is the reference temperature and the μ^* is the reference dynamic viscosity, which can be calculated from Eq. 18.

After the calculation of all variables presented above it is possible to obtain the heat transfer rate over the surface by the Eckert's reference temperature methodology given by Equation 16.

3. RESULTS AND DISCUSSIONS

The temperatures higher than 400K cause a change in thermodynamic parameters such as the specific heat at constant pressure c_p and the ratio of specific heats γ ; in comparison with calorically perfect gas assumption. Considering the air in chemical equilibrium, the thermodynamic properties over the 14-X waverider regions (Figure 2) will assume different values of that encountered by calorically perfect gas approach. In this way, using the air equilibrium module of the software HAP (Hypersonic Airbreathing Propulsion) we can obtain the property distribution along of 14-X waverider, as shown in the Figure 3a for Mach number 7 and Figure 3b for Mach number 10.

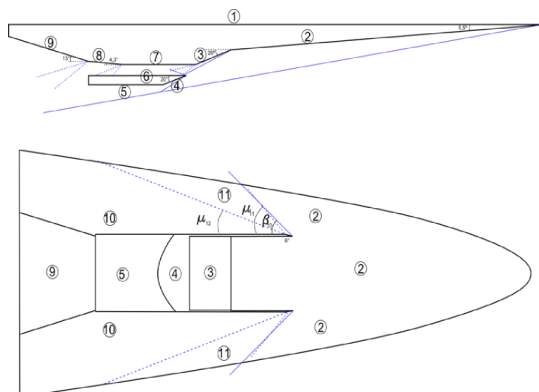


Figure 2. 14-X waverider arbitrary regions for Analytical Theoretical Analysis

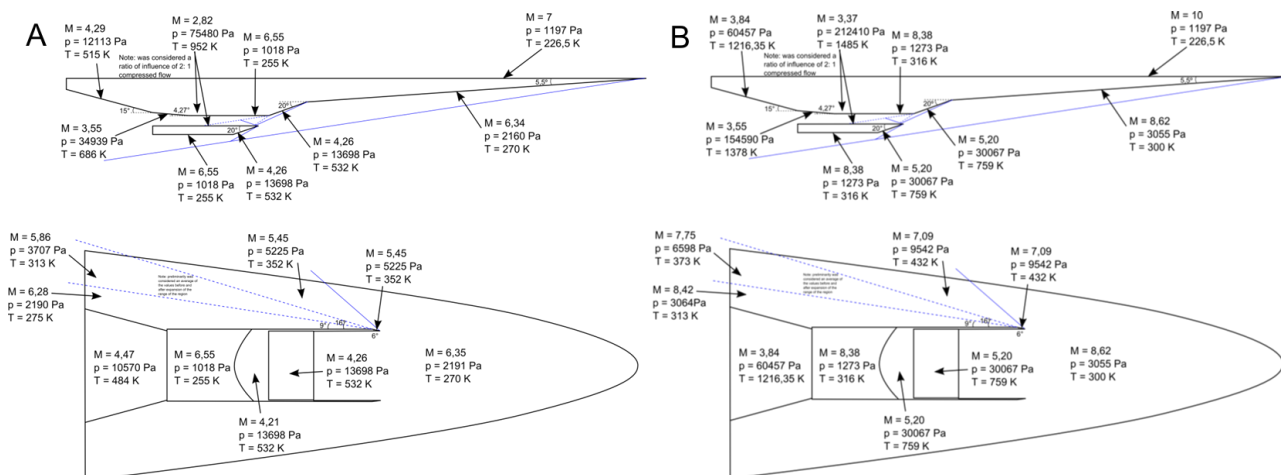


Figure 3. a) Property distribution assuming air in chemical equilibrium of the VHA 14-X at 30 km altitude at Mach 7, b) Property distribution assuming air in chemical equilibrium of the VHA 14-X at 30 km altitude at Mach 10

First of all, the atmospheric thermodynamic properties at the altitude of interest (at 30 km altitude) and the problem given data need to be known (Table 1).

Table 1. Thermodynamic air properties at 30 km of altitude and problem given data

PROBLEM GIVEN DATA		AIR PROPERTIES AT 30 Km ALTITUDE	
Nose Radius	0.05 m	Speed of Sound	301.7 m/s
Altitude	30 Km	Temperature	226.5 K
Wall Temperature	300 K	Density	$1.84 \cdot 10^{-2} \text{ kg/m}^3$
γ	1.4	Pressure	1197 Pa
R	287		
Mach Number (M_I)	7		
Speed at Mach 7	2111.9 m/s		
Mach Number (M_I)	10		
Speed at Mach 10	3017 m/s		

Applying Fay and Riddell theory at the stagnation point where the nose radius of the vehicle is 0.05 m, and considering the mission profile at 30 km of altitude and Mach number 7, the heat flux at stagnation point can be obtained as show in the Table 2.

Table 2. Heat Flux at Stagnation Point

Mach number	Heat flux [W/m^2]
7	692,345.3238
10	2,140,013.9574

The heat flux in the lower, upper, scramjet compression and expansion ramps, and scramjet fins (side wall) is provided by Eckert's reference enthalpy theory. To aerodynamic heating is needed to take in account the Reynolds number for each coordinates presented in the Figure 4. This procedure assumes instantaneous heat transfer to the vehicle structure, which provides a higher heat flux. This situation represents a conservative assumption, because not occurs in real world.

Solving the equations 13, 17, 18, 19, 24 and 25 by iteration with HAP (air module), and considering the air in chemical equilibrium it is possible to obtain the reference temperature T^* by equation 16 and hence the parameters as Prandtl number, recovery factor, Reynolds number, density and c_p could be computed for each coordinate presented in Figure 3. Finally, based on the reference temperature and parameters mentioned above, the heat flux per region (Figure 2) and coordinates (Figure 4) are presented in the Tables 3 to 5.

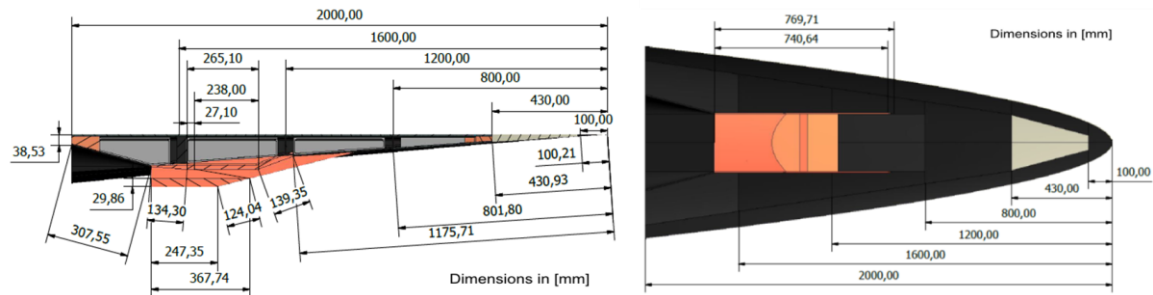


Figure 4. The Coordinates at the upper surface, the lower surface and scramjet centerline of the VHA 14-X

Table 3. Heat flux by coordinates in region 1 of the 14-X vehicle

q_1 [W/m ²]	Coordinates [m]					
Mach	0.1	0.43	0.8	1.2	1.6	2
7	47061.6	22695.1	16638.7	13585.5	11765.4	10523.2
10	80590.9	38864.3	28493.1	23264.5	20147.7	18020.6

Table 4. Heat flux by coordinates in region 2 of the 14-X vehicle

q_2 [W/m ²]	Coordinates [m]			
Mach	0.1	0.43	0.8	1.17295
7	58202.5	28066.8	20576.1	16992.1
10	130352.1	62859.4	46083.0	38056.0

Table 5. Heat flux over the VHA 14-X vehicle regions

Mach	$q_{3,4}$ [W/m ²]	q_5 [W/m ²]	$q_{6,7}$ [W/m ²]	q_8 [W/m ²]	q_9 [W/m ²]	q_{10} [W/m ²]	q_{11} [W/m ²]
7	115021	176595	103744.4	125358.4	57325.7	165383.9	18645.2
10	38849.2	47898	12324.6	473745.9	221441.6	382168.8	77732.1

The heat flux over the upper (Figure 5a) and lower (Figure 5b) surfaces of the VHA 14-X are presented for speeds corresponding to Mach numbers 7 and 10, respectively. In the lower surface, the first expansion ramp (4.27°) shows the maximum heating flux for both cases, where for Mach number 7 the heat flux magnitude is 125,358.4673 W/m², and for Mach number 10 is 473,745.9684 W/m². In the upper surface the maximum heat flux value is concentrated near to the leading edge of the VHA 14-X vehicle, where the heat flux magnitude are 47,061.6022 W/m² and 80,590.9257 W/m² for Mach number 7 and 10, respectively. It is evident that the heat flux at the upper surface decrease along the length of the vehicle, thus, we have an asymptotic curve, which agrees with the theory of aerodynamic heating over a flat plate. Comparing the heat fluxes at the lower surface, presented in the Figure 5b, we may see a proportional behavior of the heat flux up to the scramjet compression ramp with deflection of 14.5°. Taking in account the Mach number 7 case, is notable the increasing of the heat flux, after the scramjet compression ramp, due to the reflected oblique shock wave, quite constant inside of the combustor and a decreasing in the nozzle section. In other hand, the heat flux has an expressive increasing after the reflected oblique shock wave and decreasing after the scramjet engine considering the

Mach number 10 case. There is a great gap when we compare the maximum heat flux of Mach number 10 and 7 cases in the first scramjet expansion ramp and a proportional decreasing on the second expansion ramp.

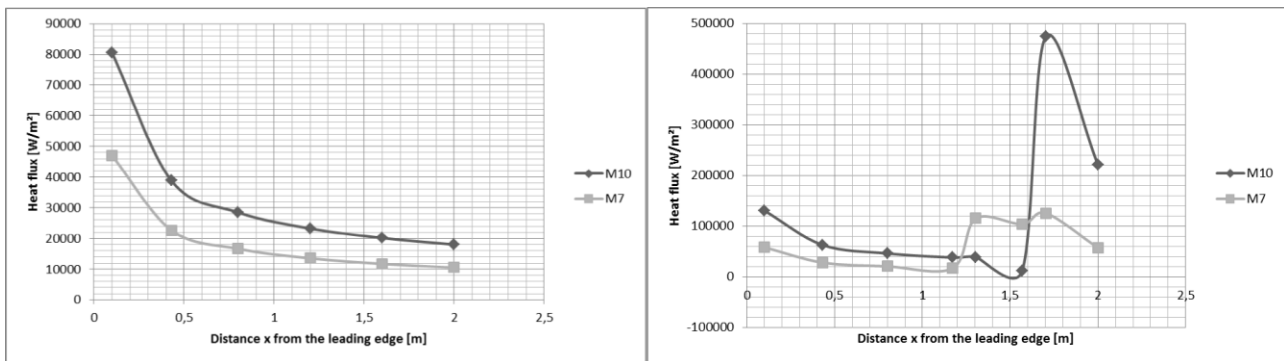


Figure 5. a) Heat Flux by Eckert's Reference Enthalpy over the VHA 14-X upper surface at Mach number 7 and 10, b) Heat Flux by Eckert's Reference Enthalpy over the VHA 14-X lower surface at Mach number 7 and 10.

3. CONCLUSIONS

Hypersonic flight introduces extreme thermal loads on the leading edges of the vehicle, which generates high temperature around the vehicle surfaces. Consequently, high temperature materials and high temperature coatings should be employed. The extreme thermal loads on the leading edges of the vehicle have a magnitude significant in terms of heat flux. The heat flux increases inversely to square root of the nose radius, as stagnation heat transfer theory, developed by Fay and Riddell. For a large leading edge radius one may obtain a lower heat flux, but several airbreathing vehicles require a small nose radius and therefore, the heat flux is significantly high. The aerodynamic heating at the stagnation point is presented in the table 2 for Mach numbers 7 and 10. The Eckert's Reference Enthalpy theory provided the aerodynamic heating over the upper and lower surfaces of the VHA 14-X and in this case the temperature, of the layer that blankets the vehicle surface, increases with the square of the speed.

5. ACKNOWLEDGEMENTS

The second author would like to express gratitude to FAPESP (project n° 2004/00525-7), to FINEP (agreement n° 01.08.0365.00, project n° 0445/07), to CNPq (project n° 471345/2007-5), to AEB (project n° 25/2009-1) for the financial support for the VHA 14-X design and experimental investigations; and to CNPq (project n° 520017/2009-9) for the financial support to undergraduate students, respectively. Also, the first author acknowledges the CNPq (grant # 183245/2009-1) for the financial support to undergraduate student.

6. REFERENCES (Times New Roman, 10pt, bold, upper-case)

- Costa, F.J., 2014. Thermo-Structural Analysis of the Brazilian 14-X Hypersonic Aerospace Vehicle. Master thesis, Instituto Tecnológico de Aeronáutica, São José dos Campos, Brazil.
- Driest, E.R., 1956. The Problem of Aerodynamic Heating. *Aeronautical Engineering Review*, p 26-41.
- Eckert, E.R.G., April, 1954. Survey on Heat Transfer at High Speeds. WADC Technical Report, p 54-70.
- Fay, J.A. and Riddell, F.R., 1958. Theory of Stagnation Point Heat Transfer in Dissociated Air. *Journal of The Aeronautical Sciences*.
- Heiser, W.H. and Pratt, D.T., 1995. Hypersonic Air breathing Propulsion. - Wright Patterson Air Force Base, Ohio, 1st Edition.
- Nielsen, J.N., 1960. Missiles Aerodynamics. McGraw-Hill Book, New York, 1st Edition.
- Lees, L., 1956. Laminar Heat Transfer Over Blunt-Nosed Bodies at Hypersonic Flight Speeds. *Jet propulsion*. Vol.26, n. 4, p 259-274
- Rubens, M.W. and Johnson, H.A., 1949. A Critical Review of Skin-friction and Heat-transfer Solutions of the Laminar Boundary Layer of a Flat Plate. *Tans. ASME*, vol. 71, n. 4, pp. 385-388.
- Sommer, S.C. and Short, B.J., Mach, 1955. Free-flight Measurements of Turbulent Boundary-layer Skin Friction in the Presence of Severe Aerodynamic Heating at Mach Numbers from 2.8 to 7.0. NACA Tech. Notes 3391

7. RESPONSIBILITY NOTICE

The authors are the only responsible for the printed material included in this paper.